AAEC/E581

AAEC/E581

AUSTRALIAN ATOMIC ENERGY COMMISSION

RESEARCH ESTABLISHMENT

LUCAS HEIGHTS RESEARCH LABORATORIES

THE EFFECT OF THE BORE HOLE ON NUCLEAR LOGGING MEASUREMENTS

by

B.J. McGREGOR
P. EISLER*

*CSIRO Division of Mineral Physics, Port Melbourne, Victoria

December 1983

ISBN 0 642 59787 1

AUSTRALIAN ATOMIC ENERGY COMMISSION
RESEARCH ESTABLISHMENT
LUCAS HEIGHTS RESEARCH LABORATORIES

THE EFFECT OF THE BORE HOLE ON NUCLEAR LOGGING MEASUREMENTS

by

B.J. McGREGOR
P. EISLER*

ABSTRACT

Measured neutron and gamma-ray fluxes in a bore hole had been successfully correlated with iron ore grades to yield the coefficients of an empirical expression which was in turn used to derive the ore grade from neutron and gamma-ray measurements in other bore holes in the same general area. The aim of the present study was to put the method on a sounder theoretical basis and to establish the simplest representation which would give reliable predictions for a wide range of field conditions without resort to empirical correlations.

(Continued)

* CSIRO Division of Mineral Physics, Port Melbourne, Victoria.

This report presents an analytical study, with sand representing an ore, to find whether the ratio of the characteristic gamma-ray flux to thermal neutron flux can be reliably used as a measure of the characteristic element, particularly if the water content of the ore is unknown. Both Monte Carlo and two-dimensional transport theory methods were used and found to be in good agreement, but the use of 2D transport theory is preferred for speed. A homogeneous analysis, which ignores the effect of the bore hole and probe, is compared to the detailed representation.

It is shown that, when the bore and probe are represented in the analysis, there is a significant variation with water content of the ratio of the characteristic gamma-ray flux to the thermal neutron flux. This variation is not accurately predicted by the homogeneous model, which is therefore inadequate.

National Library of Australia card number and ISBN 0 642 59787 1

The following descriptors have been selected from the INIS Thesaurus to describe the subject content of this report for information retrieval purposes. For further details please refer to IAEA-INIS-12 (INIS: Manual for Indexing) and IAEA-INIS-13 (INIS: Thesaurus) published in Vienna by the International Atomic Energy Agency.

BOREHOLES; EPITHERMAL NEUTRONS; GAMMA RADIATION; HUMIDITY; MONTE CARLO METHOD; NEUTRON FLUX; NEUTRON-GAMMA LOGGING; NEUTRON-NEUTRON LOGGING; SAND; THERMAL NEUTRONS; TRANSPORT THEORY; WATER

CONTENTS

1. INTRODUCTION 1

2. BORE HOLES IN SAND 3

3. METHODS 3

4. RESULTS 4
   - 4.1 Series I - Comparison of DOT and MORSE for Saturated Sand 4
   - 4.2 Water in the Hole 5
   - 4.3 Series II - Comparison of Fluxes and Flux Ratios in the Empty Hole to those Inside the Sand and to the Homogeneous Values 6
   - 4.4 Large Hole - 30.48 cm Diameter 9
   - 4.5 Series III - Spectra in Water Filled Holes 10

5. CONCLUSIONS 12

6. REFERENCES 13

Figure 1 Percentage differences between probe and interior values 15
Figure 2 Fluxes with 15 per cent saturated sand 16
Figure 3 Flux ratios 15 per cent saturated sand 17
Figure 4 Fluxes with 45 per cent saturated sand 18
Figure 5 Flux ratios 45 per cent saturated sand 19
Figure 6 Percentage differences between large hole probe and interior values 20
Figure 7 Fluxes with 15 per cent saturated sand - large hole 21

1. INTRODUCTION

Previous work [Eisler et al. 1977] has shown that the grade of an iron ore can be determined from an empirical expression involving thermal and epithermal neutron flux and the iron capture gamma-ray flux measured with a bore hole probe. The probe has a ^{252}Cf neutron source separated from the neutron and gamma-ray detector by a Bi gamma-ray shield. In general, the most important quantities measured in this type of logging are the ratio of a characteristic capture gamma-ray flux to the thermal neutron flux, which is approximately proportional to the ore grade, and the ratio of the epithermal to thermal flux, which is sensitive to the usually unknown water content of the ore. Simple analyses of bore hole measurements ignore the effects of the bore hole and shield and assume a homogeneous situation. A basic question to be considered is how close calculations of real geometries are to this homogeneous case. The relation between the ore grade and the various fluxes can be expected to depend on the probe-bore hole configuration as well as the amount of water in the hole.

Previous calculations of bore hole systems have mostly treated a water filled bore hole, allowing simple methods to be used. Nargolwalla et al. [1973] used a two-group, two-region diffusion theory similar to that found in Glasstone and Edlund [1952] with a solution involving Bessel functions. Experience with these methods has shown that the accurate programming of the Bessel functions is difficult; a finite difference solution should be more accurate. Other areas of possible error are the use of two neutron groups and the spectrum over which the two-group cross sections are derived. We repeated some of the calculations of Nargolwalla et al. for a water filled bore hole in dry and saturated sand using two- and seven-group cross sections from the AUS system [Robinson 1977] and the two-dimensional transport code DOT [Rhoades and Mynatt 1973]. There were small changes with the number of groups but the main conclusions were the same. Sand is used because it is a convenient analogue of ore material.

For large diameter empty bore holes, simple methods are inaccurate. Diffusion theory cannot handle the void and the large, fast neutron leakage from the system means that the use of one fast neutron group is inadequate, especially for dry sand.

Monte Carlo methods have previously been used to calculate the effects of the bore hole environment and water on the formation. Sanders et al. [1976]

also considered analytical and diffusion theory solutions and two-group analysis to have unknown errors. They used the Monte Carlo code McNID to quantify the effects of the bore hole conditions on the flux distribution. Starting from the basic case of a point source in an infinite medium of dry silica, a progressive study was made of the effects of 15 wt % water in the formation, two sizes of empty bore holes (6 cm and 26 cm diameter), water in the bore holes, a steel liner (3 cm thickness), and a radial boundary. Fast, epithermal and thermal (< 0.1 eV) fluxes were plotted throughout the system. Two thousand source neutrons were followed with the flux in a region being the total path length through that region. This study showed trends rather than accurate results. Large statistical errors were present, especially at detector positions in the empty bore hole cases.

A comparison was made of the results of Sanders et al. [1976] for the no bore hole case, with and without water and results obtained using the AUS codes MIRANDA (eight-group condensation) and ANAUSN (one-dimensional SN transport code in spherical geometry). The ratio between the thermal flux at 20 cm radius and that at 60 cm radius was found to be about 3 in the dry case and 200 in the wet case, which agreed with the Sanders et al. results within the statistical errors.

TABLE 1
SLOWING DOWN AND DIFFUSION LENGTHS

Material	L_S (cm)	L_D (cm)	Thermal Flux (< 0.2 eV) 5 cm	Thermal Flux (< 0.2 eV) 60 cm
Dry sand (28% porosity - ρ = 1.91)	37.1	27.5	1 900	530
100% saturated sand	8.9	7.1	45 300	42
25% saturated sand	17.7	15.6	10 700	610
Hematite	18.0	3.6	654	11
Shale	8.7	6.6	45 000	30
Graphite	17.3	60.3	25 000	4 340
Water	4.8	2.77	116 000	0.16

As a prelude to these studies, the slowing down and diffusion lengths and the thermal flux at various distances from a ^{252}Cf point (10^7 neutrons s^{-1}) source were found using the AUS system for dry sand, 100 and 25 per cent saturated sand, hematite, shale and combinations of hematite and shale (Table 1).

2. BORE HOLES IN SAND

To examine variations from the homogeneous situations, a series of experiments is proposed to be carried out at CSIRO's, Division of Mineral Physics Laboratory. They will examine the effects on the neutron and gamma-ray fluxes of different size holes through a cylinder of sand and with various water contents. The holes will be either empty or full of water. Fluxes will be measured at the detector position in the holes and at corresponding positions inside the sand. The measurements inside the sand should approximate the homogeneous situation for small, voided bore holes.

To provide design information for the experiments, a theoretical study has been made of the effects of 12.7 and 30.5 cm diameter holes through a cylinder of sand with various water contents. A first series of calculations found neutron fluxes at the detector position for empty and water filled holes in a 50 cm radius, 100 cm high cylinder of saturated sand (28 per cent porosity). A second series of calculations compared important flux ratios in the empty holes to those at corresponding points inside the sand and to the homogeneous cases for three water contents of sand covering the range of water content of most host rocks. A third series was for a water filled bore hole.

3. METHODS

The first series of calculations were made with a general purpose Monte Carlo code, MORSE [Emmett 1975], and also with the two-dimensional transport theory code, DOT. Consistent with previous experience, the comparison between Monte Carlo and two-dimensional transport methods was vital in producing a reliable method of calculation with either of them. To calculate these systems with a two-dimensional transport code in a reasonable computer time, a minimum number of energy groups is used. Initial calculations showed that about eight neutron groups were required to describe accurately the slowing down process, especially in sand with low water content and consequent high neutron leakage. Comparisons were made between calculations with cross section sets condensed from the 127-group AUS library and from a coupled 22 neutron-18 gamma-ray group CASK library [RSIC, no date], with good agreement. The second series of calculations was made with CASK cross sections condensed, using the spectra appropriate to the material, into a 12-group set with 7 neutron and 5 gamma-ray groups. With this cross section set, a DOT calculation of the system requires about 10 minutes on an IBM3033S computer.

The MORSE calculations with one flux calculation position also ran for 10 minutes.

4. RESULTS

4.1 Series I - Comparison of DOT and MORSE for Saturated Sand

Comparisons were made for the homogeneous case and with the space in the hole empty and filled with water and saturated sand. The source was a 1 cm x 0.8 cm diameter cylinder inside a 9.3 cm high x 2.54 cm diameter polythene cylinder. A bismuth shield of length 20 cm and diameter 6.36 cm was immediately below the polythene cylinder. The detector, of length 5.08 cm, was on the central axis of the hole immediately below the shield; the distance from the source to the centre of the detector was 27.2 cm. Results are for this detector position (see Figure 2 for the source-shield-detector setup).

Five energy groups were used for the series; this was adequate because of the high water content of the sand (saturated, 28 per cent porosity, assumed zero porosity density 2.65). Fluxes at the detector are given for three neutron energy ranges: fast, > 0.457 eV, epithermal, 0.206 to 0.45 eV and thermal, < 0.206 eV (Table 2).

TABLE 2

CASE 0 - HOMOGENEOUS -

ALL SATURATED SAND - NO HOLE OR SHIELD

	DOT	MORSE/DOT Ratio
Fast	8.86-5*	0.97 (3%)
Epithermal	6.73-6	0.89 (20%)
Thermal	3.40-4	0.98 (1.4%)

* 8.86-5 denotes 8.86×10^{-5}

Results are for one source neutron per second. The MORSE standard deviation is given as a percentage after the MORSE/DOT ratio. The two methods of calculation are in good agreement within the Monte Carlo statistical error bounds. The large standard deviation on the epithermal flux is due to the narrow width of the group (Table 3).

TABLE 3
CASE 1 - VOID IN HOLE -
VALUES ON THE CENTRAL AXIS AT DETECTOR LEVEL

	12.7 cm hole		30.48 cm hole	
	DOT	MORSE/DOT	DOT	MORSE/DOT
Fast	2.21-4	0.96 (4%)	1.97-4	1.06 (3%)
Epithermal	1.23-5	0.94 (7%)	8.96-6	1.01 (7%)
Thermal	4.57-4	0.93 (5%)	2.29-4	1.13 (8%)

Agreement between MORSE and DOT is satisfactory. The flux is increased compared to the homogeneous case for all energies with the 12.7 cm hole, and for fast and epithermal energies with the 30.48 cm hole. The thermal flux decreases in the large hole. There are two competing effects of the empty hole on the thermal flux at the detector. One is that high energy source neutrons leak from the system through the hole and hence have the effect of reducing all flux levels including the thermal flux at the detector. The hole also provides a path for neutrons to travel with fewer collisions to the vicinity of the detector, thus increasing the thermal flux by an amount depending on the quantity of water present in the sand. For this saturated sand system, the thermal flux increased with the 12.7 cm hole and decreased with the 30.48 cm hole. The variation is a function of detector position.

4.2 Water in the Hole

Monte Carlo calculations at a point use a next collision flight estimator. With water in the hole the errors in estimating the fluxes on axis were too large. (Recent work on point estimation has shown that the error could be reduced by sampling whether to include the effects of a collision depending on the collision-detector distance.) Comparisons were made between fluxes averaged over the area of the hole at the detector level. Axial DOT values are given for comparison with the homogeneous and void hole cases (Table 4).

MORSE and DOT are in agreement within the larger statistical errors. Compared to the homogeneous case, the fast and epithermal fluxes are depressed. Comparison of the DOT axial values with those averaged over the holes shows a definite peaking in the thermal flux on the axis. Cases were also run with saturated sand in the hole. All flux values at the detector were higher than for the homogeneous case, since bismuth is a poorer neutron

shield than saturated sand.

TABLE 4
CASE 2 - WATER IN HOLE
FLUXES AVERAGED OVER AREA OF HOLE AT DETECTOR LEVEL

	12.7 cm hole			30.48 cm hole		
	DOT	MORSE/DOT	Axial DOT	DOT	MORSE/DOT	Axial DOT
Fast	4.45-5	0.93 (20%)	4.49-5	1.03-5	1.34 (23%)	2.33-5
Epithermal	3.94-6	1.22 (35%)	4.61-6	9.20-7	0.96 (52%)	2.66-6
Thermal	2.85-4	0.85 (10%)	3.71-4	9.60-5	0.91 (17%)	2.44-4

This series of calculations showed that both Monte Carlo and two-dimensional transport methods can be used to calculate the system with empty holes. The choice of method to use depends on the number of points where the flux is required and the number of energy groups required to accurately represent the slowing down process. The computer time for the Monte Carlo method is sensitive to the number of flux points required, whereas the time for the two-dimensional transport method is strongly dependent on the number of groups. The second series of calculations required the flux at a number of points in 12 energy groups. The two-dimensional code, DOT, was the better method. The large statistical errors with the Monte Carlo calculation of the water filled hole make accurate calculations with this procedure difficult without the use of variance reducing techniques. Overall, the use of the DOT code seems the preferred method. From then on, DOT was used. When measured, the dry sand density was found to be 1.80 g cm^{-3} (porosity 32 per cent). The 6 per cent density change would alter the calculated results but this would have little effect on the DOT/MORSE comparison.

4.3 Series II - Comparison of Fluxes and Flux Ratios in the Empty Hole to those Inside the Sand and to the Homogeneous Values

This series of calculations compared important flux ratios at the detector position in empty holes to those at corresponding positions inside the sand and also to the homogeneous case. Table 5 gives the value of the important fluxes, epithermal (6), thermal (7) and silicon gamma-ray (9) at two positions in the 12.7 cm hole for 32 per cent porosity sand and for five water contents, i.e. dry, 15, 30, 45 and 100 per cent of the porous component. The range 15 to 45 per cent, which corresponds to 2.7 to 8.0 per cent of the dry density (1.8 g cm^{-3}), covers the range of water contents of most host rocks

and is the range of greatest interest in this study. The dry and saturated cases illustrate what happens if extrapolations are made outside this range.

TABLE 5

SPECTRA IN 12.7 cm HOLE AND COMPARISON WITH HOMOGENEOUS CASE

	Group	Dry	32-15	32-30	32-45	Saturated
A. Spectra at 27.2 cm below source in 12.7 cm hole						
Epithermal	6	2.93-6	1.36-5	1.38-5	1.29-5	9.87-6
Thermal	7	7.13-6	1.64-4	3.02-4	3.79-4	4.64-4
Real	6/7	0.411	0.083	0.046	0.034	0.021
Homogeneous	6/7	0.445	0.078	0.041	0.027	0.0121
Ratio (Real/Homo)		0.92	1.06	1.12	1.26	1.73
Gamma-ray	9	8.05-7	7.91-6	1.31-5	1.55-5	1.47-5
Real	9/7	0.113	0.048	0.043	0.041	0.032
Homogeneous	9/7	0.140	0.057	0.054	0.054	0.062
Ratio (Real/Homo)		0.81	0.84	0.80	0.76	0.52
B. Spectra at 33 cm below source in 12.7 cm hole						
Epithermal	6	2.51-6	1.13-5	1.11-5	1.01-5	7.37-6
Thermal	7	6.13-6	1.37-4	2.47-4	3.04-4	3.53-4
Real	6/7	0.409	0.082	0.045	0.033	0.021
Homogeneous	6/7	0.442	0.074	0.036	0.023	0.0098
Ratio (Real/Homo)		0.93	1.11	1.25	1.44	2.13
Gamma-ray	9	7.59-7	7.56-6	1.25-5	1.46-5	1.37-5
Real	9/7	0.124	0.055	0.051	0.048	0.039
Homogeneous	9/7	0.133	0.058	0.057	0.058	0.079
Ratio (Real/Homo)		0.93	0.95	0.89	0.83	0.49

Examining Table 5 (27.2 cm), it can be seen that the epithermal flux (group 6) is fairly constant across the important water content range. The thermal flux is nearly proportional to the water content and the gamma-ray flux (group 9) to the first approximation follows the thermal flux. The important flux ratios are the silicon gamma-ray/thermal ratio, which is nearly proportional to the amount of ore (in this case, silicon) present, and the epithermal/thermal ratio, which is a measure of the usually unknown water content of the ore. The silicon gamma/thermal ratio is nearly constant from 15 to 45 per cent saturation in the homogeneous case, but decreases with increasing saturation in the real case. The ratio between the real and homogeneous cases varies from 0.84 to 0.76. The epithermal/thermal ratio in

the hole is larger than the homogeneous case for 15 per cent saturation and the ratio between the real and homogeneous cases increases with increasing saturation.

Similar effects are seen with a detector at 33 cm. A better probe design would be one in which the gamma-ray/thermal flux ratio varied less with water content. Using this criterion, the 33 cm source detector separation is slightly better for the gamma-ray/thermal ratio although the changes with water content from the homogeneous ratios are increased.

TABLE 6
RATIO OF FLUX AT INTERIOR POINT TO THAT IN THE HOLE (12.7 cm)

R	Dry	32-15	32-30	32-45	Saturated
Epithermal Flux (6)					
25	1.29	1.32	1.30	1.23	0.85
27	1.21	1.21	1.11	1.05	0.65
29	1.19	1.15	1.06	0.93	0.50
33	1.16	1.08	0.93	0.76	0.39
Thermal Flux (7)					
25	1.30	1.33	1.32	1.31	1.04
27	1.22	1.24	1.19	1.19	0.82
29	1.20	1.21	1.16	1.11	0.72
33	1.16	1.17	1.08	0.98	0.51
Silicon Gamma-ray Flux (9)					
25	1.95	2.2	2.3	2.5	2.5
27	1.39	1.47	1.47	1.50	1.39
29	1.24	1.31	1.29	1.28	1.08
33	1.15	1.22	1.18	1.14	0.85

Table 6 shows the variation at the same source-detector distance, R, in the ratio of the flux at a typical interior point to that in the hole for the five water contents and four source-detector distances. The typical point is a point equidistant from the source and detector (see Figure 2). In the range 15 to 45 per cent, the ratio generally decreases with increasing water content and with increasing source-detector distances. The large ratios at R = 25 for the silicon gamma-ray flux are caused by shadowing by the gamma-ray shield. Figure 1 illustrates the variation with water content of the percentage difference between the probe (in hole) and interior values for the two flux

ratios of greatest interest. For the epithermal to thermal ratio, the probe values increase with increased water content relative to the interior values, whereas the reverse is true for the gamma-ray to thermal ratio. The effect of the hole varies with water content of the ore.

Figure 2 shows the angular variation of the thermal and silicon gamma-ray fluxes at two source-detector distances (27 and 33 cm) for 15 per cent saturated sand. Values are given at r = 0, z = ± 27.2 and ± 33.0 cm, at z = 0, r = 0, 27.2 and 33.0, and at the typical interior points at z = -13.6, r = 23.6 (27.2 radius) and z = -16.5, r = 28.6 (33.0 radius). The 27 cm value corresponds to the centre of the detector which is positioned adjacent to the shield. At this position in the hole, the gamma-ray shield is reducing the gamma-ray flux. All fluxes are less than the corresponding homogeneous values.

Figure 3 shows the flux ratios for the same case. There is much less variation than with the individual fluxes. The gamma-ray/thermal ratio is almost constant at the homogeneous values, except at the probe in the hole. Figure 4 shows fluxes for the 45 per cent saturated sand. The thermal values on the far side of the hole from the detector are now higher than the interior values and about 20 per cent higher than the values at the detector position. For the saturated sand case, this difference rose to 40 per cent which seemed anomalous, but a Monte Carlo recalculation confirmed this result. With the increased water content, the ratio of 33 to 27 cm fluxes decreased. Figure 5 completes the 12.7 cm void hole results with the flux ratios for the 45 per cent saturated sand.

4.4 Large Hole - 30.48 cm Diameter

A slightly wider shield (7.62 cm diameter) was assumed in the larger hole. Table 7 shows the spectra at the detector adjacent to the shield. Compared to the 12.7 cm hole results (Table 5), fluxes are decreased by a factor of about 2.5 because of the increased leakage. The variations in the epithermal and thermal neutron and gamma-ray fluxes with changing saturation are similar to those in the 12.7 cm hole. The epithermal/thermal ratios are increased compared to the small hole values, but importantly the gamma-ray/thermal ratios are very similar for saturations above 15 per cent (2.7 wt %).

TABLE 7
SPECTRA IN 30.5 cm HOLE AND COMPARISON WITH HOMOGENEOUS CASE

Source-Detector Distance 27.2 cm						
	Group	Dry	32-15	32-30	32-45	Saturated
Epithermal	6	7.97-7	6.29-6	7.26-6	7.35-6	6.92-6
Thermal	7	1.56-6	6.04-5	1.20-4	1.63-4	2.27-4
Real	6/7	0.51	0.104	0.061	0.045	0.030
Homogeneous	6/7	0.45	0.078	0.041	0.027	0.0121
Ratio (Real/Homo)		1.14	1.34	1.48	1.67	2.5
Gamma-ray	9	2.81-7	2.90-6	5.30-6	6.81-6	7.84-6
Real	9/7	0.180	0.048	0.044	0.042	0.035
Homogeneous	9/7	0.140	0.057	0.054	0.054	0.062
Ratio (Real/Homo)		1.29	0.84	0.82	0.77	0.55

Figure 6 shows the percentage differences between probe (hole) and interior values. The epithermal/thermal results show similar trends to those for the 12.7 cm hole. However, for source-detector distances of 29 and particularly 33 cm, the gamma-ray/thermal ratio is nearly the same at the interior points as it is at the hole. The ratio at the interior points always lies between the value at the probe in the hole and the homogeneous value. For the 12.7 cm hole, the interior point ratios were closer to the homogeneous values, but for the larger hole they are very close to the values in the hole.

The flux values for the large hole in 15 per cent saturated sand are shown in Figure 7. The epithermal and thermal fluxes are shown since the gamma-ray/thermal ratios are nearly constant. Comparing the thermal values with those for the small hole (Figure 2), the ratio of small hole/large hole is about 2.6 at the detector position and in the hole on the far side from the source, whereas interior values are closer to 2.0.

4.5 Series III - Spectra in Water Filled Holes

A third series of calculations dealt with the flux values and ratios when the holes were filled with water. Table 8 shows the spectra at the detector position in the hole for a water filled 12.7 cm hole. Results are given for two source-detector distances of 27.2 cm and 32.8 cm and five water contents. The thermal flux in the water filled hole decreases as the water content in the surrounding sand increases. The epithermal flux decreases at a faster

rate while the silicon gamma-ray flux increases and peaks at 30 per cent saturation. There is a large increase in the gamma-ray/thermal flux ratio when moving from 27.2 cm to 32.8 cm source-detector distance owing to the rapid change in the thermal flux. The gamma-ray flux is nearly constant in the 15-45 per cent saturation range and appears to be a better choice than the gamma-ray/thermal ratio for water filled holes. As was expected, there is little correlation with the results for the empty hole or the homogeneous situation.

TABLE 8
SPECTRA IN WATER FILLED 12.7 cm HOLE

	Group	Dry	32-15	32-30	32-45	Saturated
Source-Detector Distance 27.2 cm						
Epithermal	(6)	6.25-6	4.50-6	3.59-6	3.05-6	2.14-6
Thermal	(7)	4.74-4	4.24-4	3.87-4	3.55-4	2.77-4
	6/7	0.0132	0.0106	0.0093	0.0086	0.0077
Gamma-ray	(9)	6.32-6	9.57-6	1.05-5	1.01-5	6.72-6
	9/7	0.0133	0.0226	0.0271	0.0285	0.0243
Source-Detector Distance 32.8 cm						
Epithermal	(6)	2.97-6	1.80-6	1.24-6	9.36-7	4.96-7
Thermal	(7)	2.37-4	1.82-4	1.45-4	1.17-4	6.28-5
	6/7	0.0125	0.0099	0.0086	0.0080	0.0079
Gamma-ray	(9)	5.74-6	8.61-6	9.32-6	8.91-6	5.96-6
	9/7	0.0242	0.0473	0.0643	0.0762	0.0949

Table 9 shows spectra at the centre of the large 30.5 cm hole filled with water. The neutron spectra at the centre of the hole are nearly independent of the water content of the material outside the hole. The silicon gamma-ray flux shows some variation with water content. The gamma-ray fluxes are reduced since a lot of the material in the system does not contain silicon.

TABLE 9
SPECTRA IN WATER FILLED 30.5 cm HOLE

	Group	Dry	32-15	32-30	32-45	Saturated
Source-Detector Distance 27.2 cm						
Epithermal	(6)	1.63-6	1.63-6	1.63-6	1.63-6	1.61-6
Thermal	(7)	2.24-4	2.26-4	2.25-4	2.25-4	2.24-4
	6/7	0.0073	0.0072	0.0072	0.0072	0.0072
Gamma-ray	(9)	9.37-7	1.21-6	1.26-6	1.21-6	9.34-7
	9/7	0.0042	0.0054	0.0056	0.0054	0.0042
Source-Detector Distance 32.8 cm						
Epithermal	(6)	2.99-7	2.95-7	2.92-7	2.90-7	2.84-7
Thermal	(7)	3.67-5	3.64-5	3.58-5	3.55-5	3.47-5
	6/7	0.0081	0.0081	0.0082	0.0082	0.0082
Gamma-ray	(9)	8.89-7	1.51-6	1.20-6	1.15-6	8.89-7
	9/7	0.0242	0.0316	0.0335	0.0324	0.0256

5. CONCLUSIONS

With this type of probe system, the simplest approximation is that the ratio of the characteristic gamma-ray flux to the thermal neutron flux is proportional to the amount of the characteristic element present in the surrounding ore body, independent of the other elements, particularly water in the ore body and bore hole. The homogeneous assumption is to ignore the effects of the bore hole and probe and assume homogeneous ore material.

If the bore hole is filled with water, both approximations are inaccurate as the gamma-ray flux rather than the ratio of the gamma-ray flux to the thermal neutron flux is nearly proportional to the amount of the characteristic element.

When the bore hole is empty, the ratio of the characteristic gamma-ray flux to the thermal neutron flux, as measured at the probe detector, shows a small but significant variation as the water content is varied within the range usually found in ores (15-45 per cent of the porous component). Although the ratio is nearly independent of water content for the homogeneous assumption, accurate analysis shows the ratio varying by about 15 per cent as the water content goes from 15 to 45 per cent, and its value is from 5 to 17

per cent lower than the nearly constant homogeneous value. The homogeneous assumption is therefore inadequate.

Knowledge of the epithermal to thermal flux ratio in an ore of unknown water content would allow the water content to be estimated approximately and a correction made to the characteristic gamma-ray to thermal flux ratio to allow for the effect of the empty bore hole.

The two-dimensional transport (e.g. DOT) calculations agree with full Monte Carlo solutions and should be used for analyses of similar experiments.

6. REFERENCES

Eisler, P.L., Huppert, P., Mathew, P.J., Wylie, A.W.. and Youl, S.F. [1977] - Use of Neutron Capture Gamma Radiation for Determining Grade of Iron Ore in Blast Holes and Exploration Holes. IAEA-SM-216/3, Vienna, March.

Emmett, M.B. [1975] - The MORSE Monte Carlo Radiation Transport Code System. ORNL-4972.

Glasstone, S. and Edlund, M.C. [1952] - The Elements of Nuclear Reactor Theory. Van Nostrand, Princeton, New Jersey.

Nargolwalla, S.S., Nguyen, N.D. and Aziz-Ur-Rehman [1977] - Nuclear Methods in Mineral Exploration and Production (ed. J.G. Morse). Elsevier Scientific Publishing, Amsterdam.

Rhoades, W.A. and Mynatt, F.R. [1973] - The DOT III Two-dimensional Discrete Ordinates Transport Code. ORNL-TM-4280.

Robinson, G.S. [1977] - AUS Module MIRANDA - A Data Preparation Code based on Multiregion Resonance Theory. AAEC/E410.

RSIC [no date] - CASK-40 Group Neutron and Gamma-ray Cross Section Data. ORNL Radiation Shielding Information Center. RSIC DLC23.

Sanders, L.G., Wormald, M.R. and Clayton, C.G. [1976] - Formation Analysis by Steady-state Neutron Interaction Techniques. AERE-R8338.

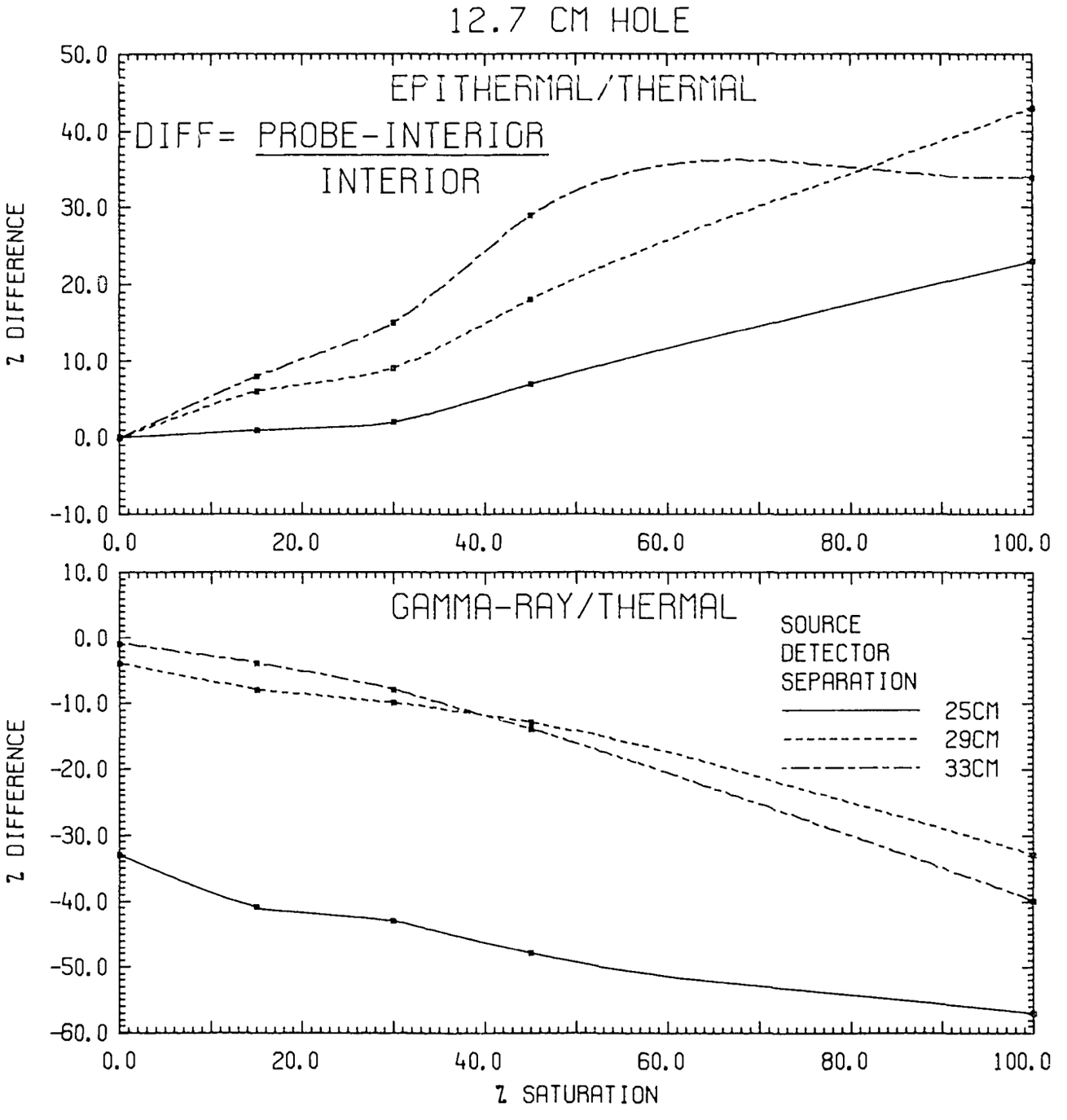

FIGURE 1. PERCENTAGE DIFFERENCES BETWEEN PROBE AND INTERIOR VALUES

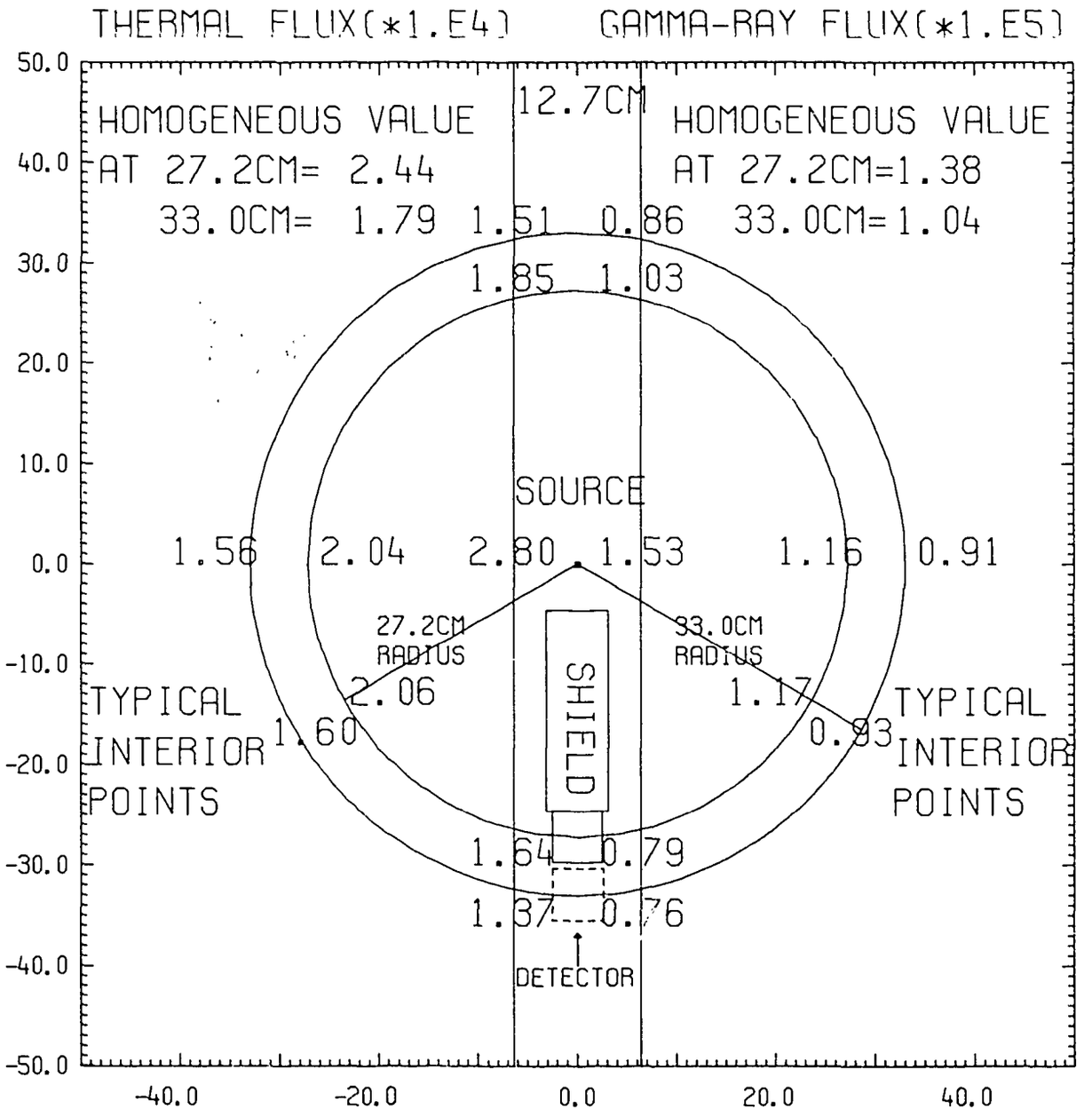

FIGURE 2. FLUXES WITH 15% SATURATED SAND

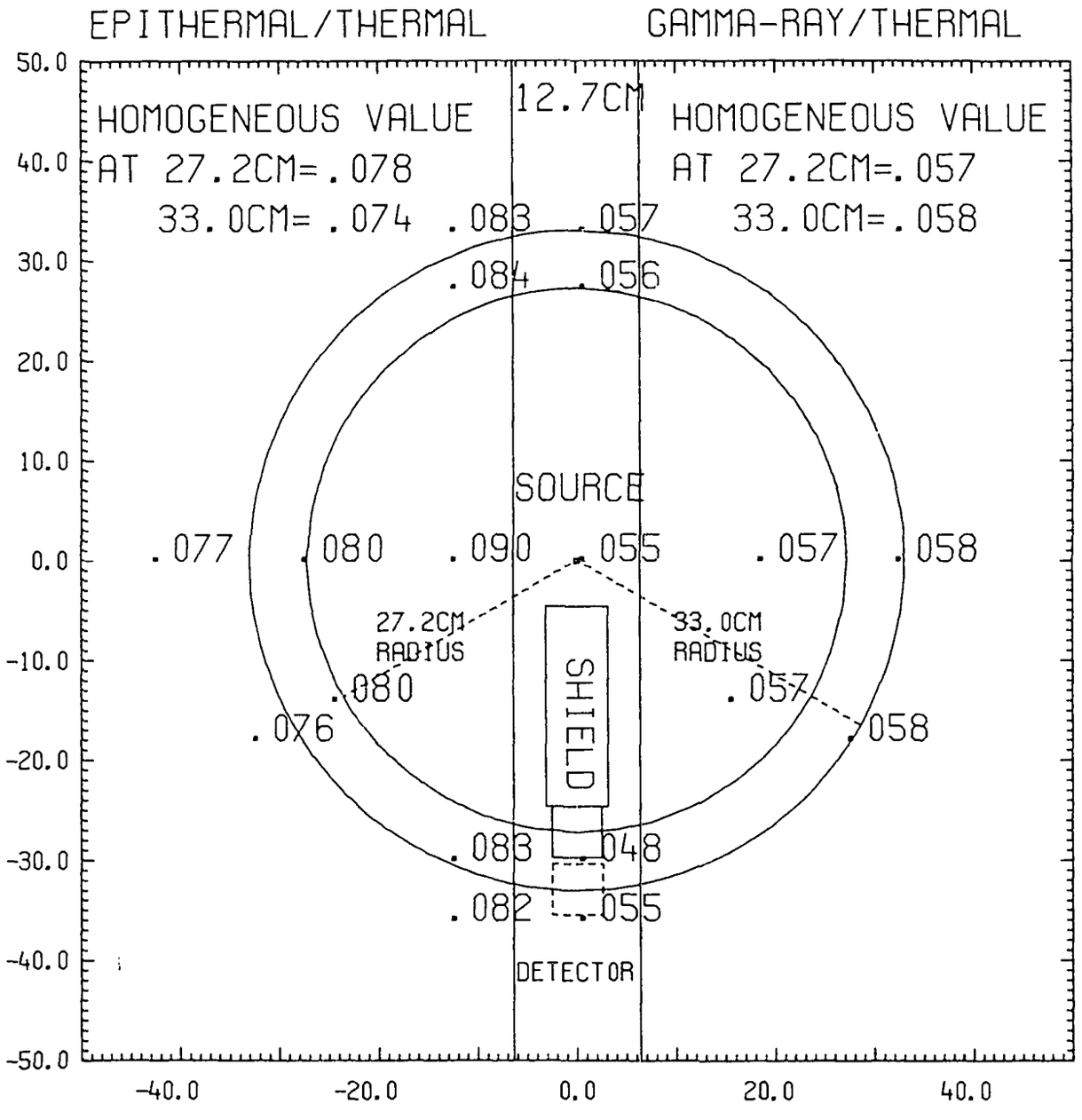

FIGURE 3. FLUX RATIOS 15% SATURATED SAND

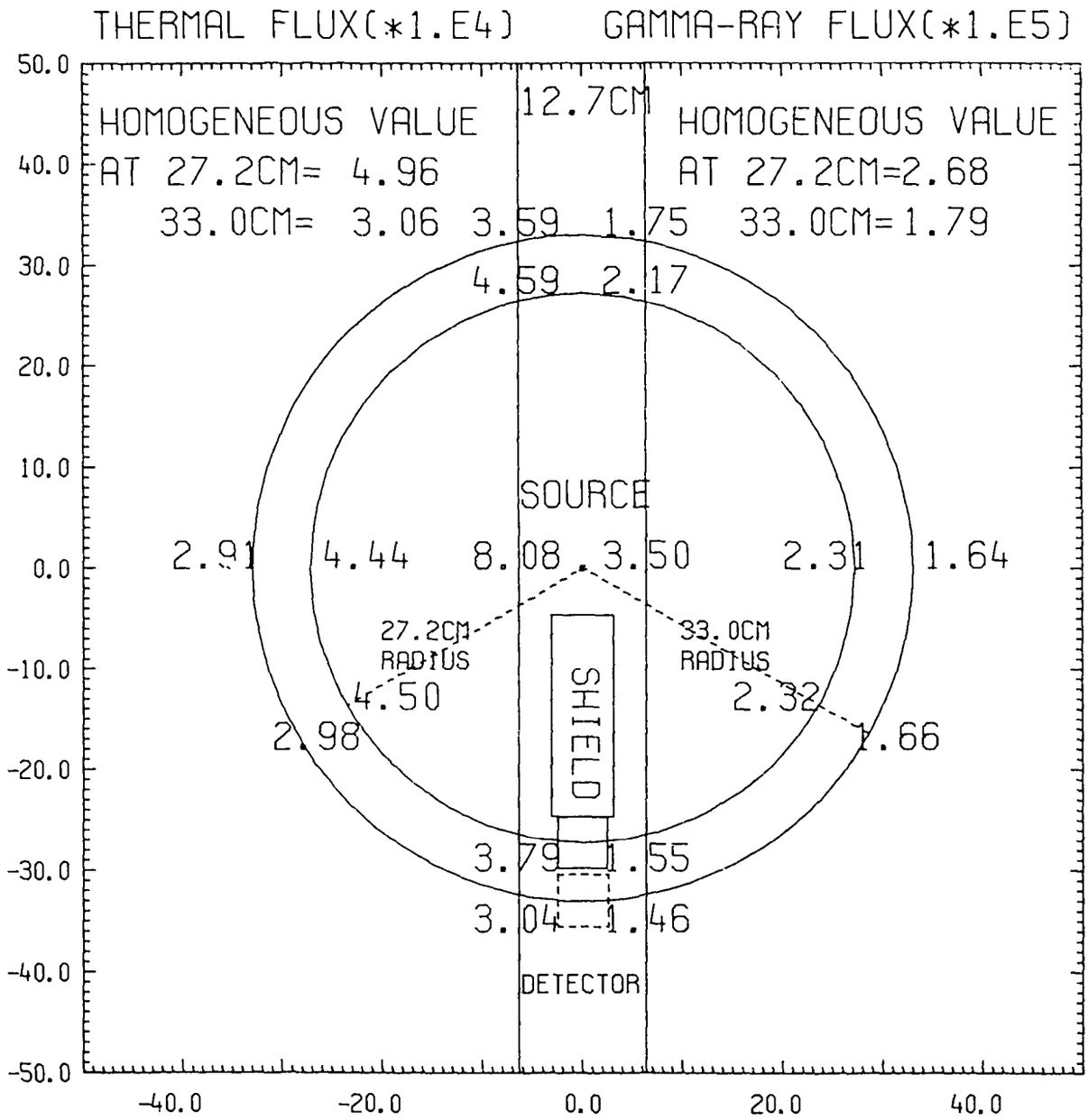

FIGURE 4. FLUXES WITH 45% SATURATED SAND

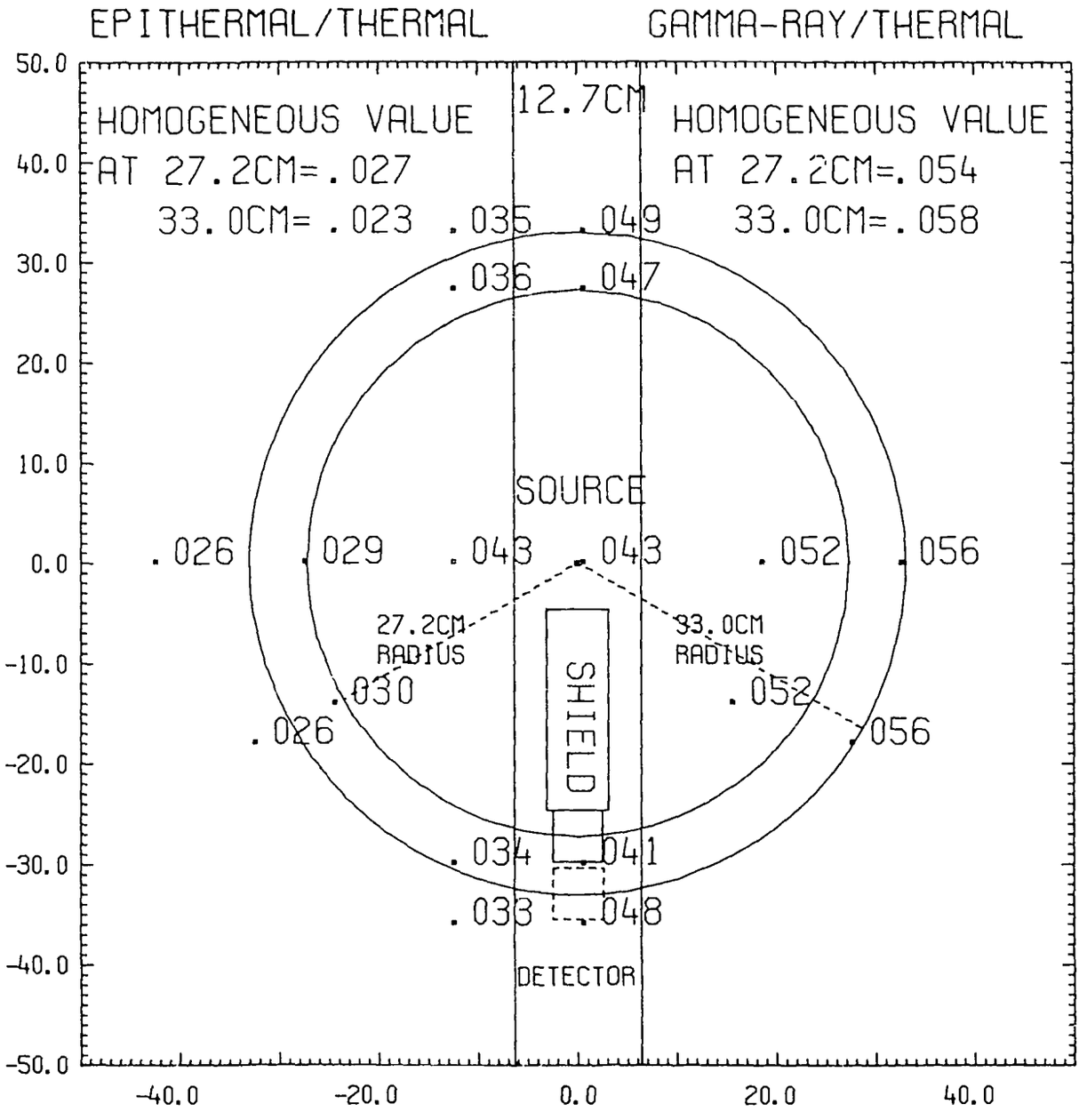

FIGURE 5. FLUX RATIOS 45% SATURATED SAND

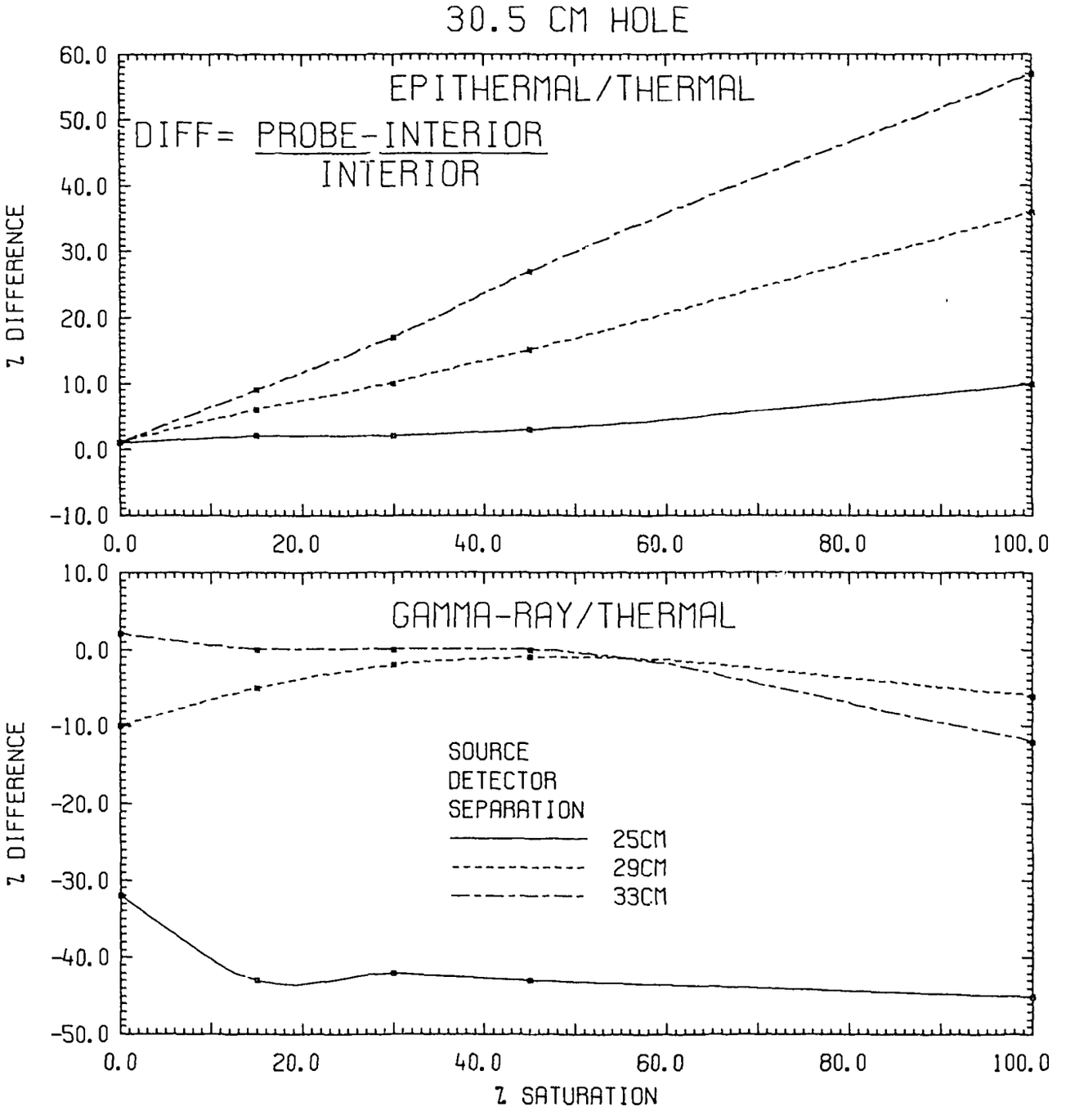

FIGURE 6. PERCENTAGE DIFFERENCES BETWEEN LARGE HOLE PROBE AND INTERIOR VALUES

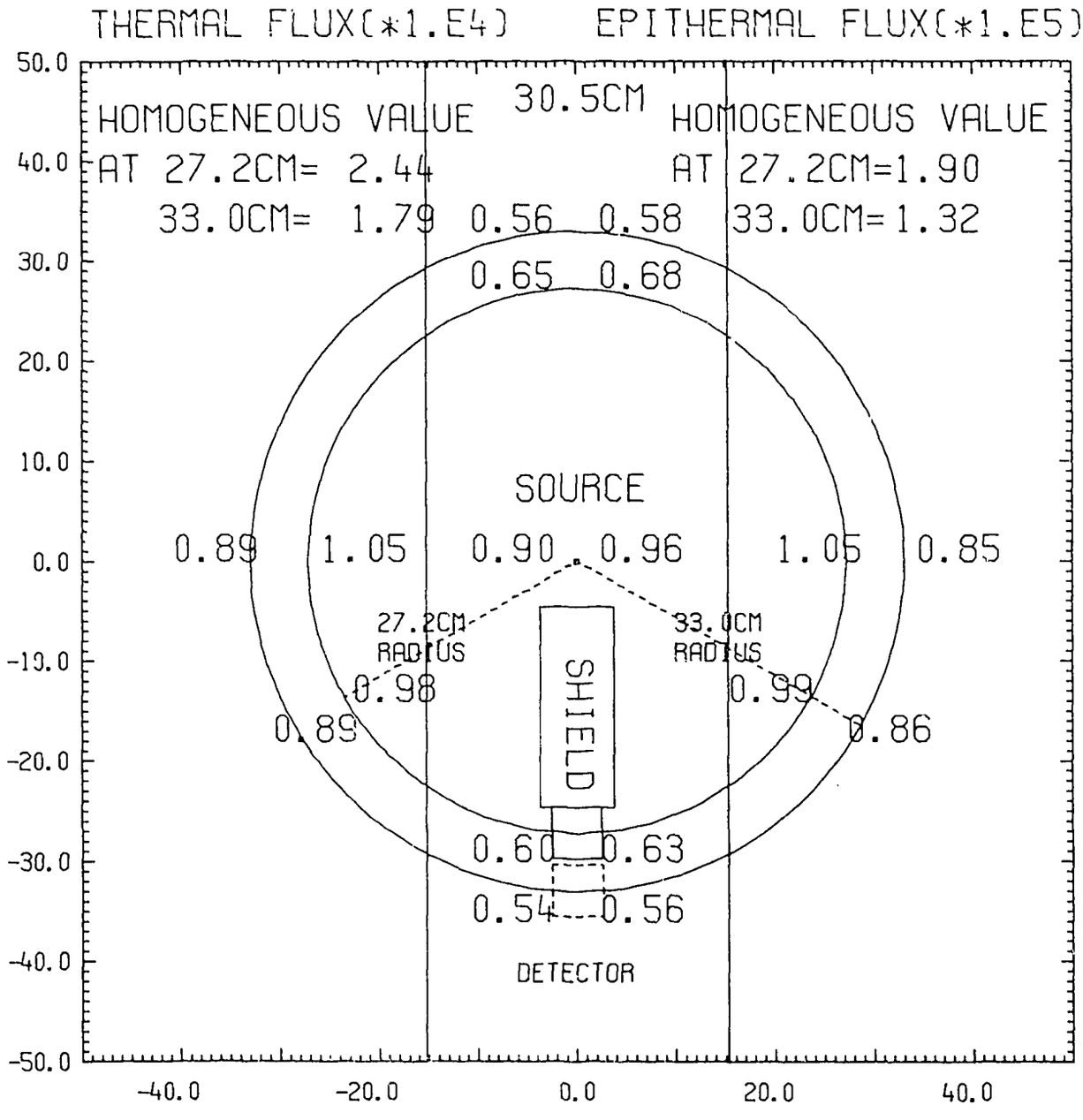

FIGURE 7. FLUXES WITH 15% SATURATED SAND - LARGE HOLE